Optica Applicata, Vol. XXXV, No. 3, 2005

Thermally induced changes of broad contact pulse-operated single quantum well (SQW) separate confinement heterostructure (SCH) laser spectra

EMIL KOWALCZYK, LESZEK ORNOCH, ANNA SZERLING, BOHDAN MROZIEWICZ

Institute of Electron Technology, al. Lotników 32/46, 02-668 Warszawa, Poland

A technique of time-resolved laser spectra mapping has been developed to assess thermo-optical properties of diode lasers. Using this technique the emission spectra of broad contact pulse operated diode lasers were measured for consecutive time points within the pulse duration width. The emitted wavelength was found to be highly dependent on the time elapsing from the pulse front and a time shift of wavelength was clearly observed in the spectrum of pulse-operated lasers.

Keywords: thermal dynamics, SQW laser, spectrum.

1. Introduction

The thermal behavior is an important parameter for achieving optimal performance of pulse-operated semiconductor diode lasers. Especially, temperature of the *p-i-n* junction enclosed in the active region plays a critical role in proper work of these lasers. The junction temperature affects laser diode performance in many ways. Most important, magnitude of the light output power and a center wavelength of the spectrum and diode reliability are strongly dependent on the temperature of the laser active region.

In general, it is possible to deduce the junction temperature from the laser threshold [1] or the spectrum envelope of the stimulated emission [2]. However, these techniques are weakly accurate and indicate low sensitivity. The thermoreflectance technique provides high sensitivity and high spatial resolution but it works well for low-power laser diodes where temperature profile within the laser is rather flat [3].

In this paper, a time-resolved technique that allows measuring laser mode spectral characteristic for an arbitrarily selected moment within the pulse duration time is presented.

2. Experiment

The laser under investigation was of a conventional ridge waveguide type with InGaAs/GaAs separate confinement heterostructure (SCH) single quantum well (SQW) structure designed for emission at 980 nm under room temperature (RT) conditions. The laser was fabricated from heterostructures molecular beam epitaxy (MBE) grown on (100) GaAs conductive substrates.

The sequence of the layers, that formed the laser, consisted an *n*-type GaAs buffer, the Si-doped $Al_{0.3}Ga_{0.7}As$ *n*-type barrier layer, the $In_{0.20}Ga_{0.80}As$ undoped quantum well located inside the GaAs waveguide, the Be-doped *p*-type $Al_{0.3}Ga_{0.7}As$ barrier layer and a *p*-type GaAs cap layer. The strained $In_{0.20}Ga_{0.80}As$ quantum well was 60 Å thick and was confined by two 0.3 μm undoped GaAs layers. Detailed data (thickness and the composition profile) describing the epitaxial structure is presented in the Table.

T a b l e. Detailed parameters of the SCH SQW InGaAs/GaAs laser structures.

Buffer	1 μm,	GaAs,	Si-doped $n = 1.5\times10^{18}$ cm^{-3}
n-type emitter	1.5 μm,	$Al_{0.3}Ga_{0.7}As$,	Si-doped $n = 1\times10^{17}$ cm^{-3}
Waveguide	0.3 μm,	GaAs,	undoped
Quantum well	60 Å,	$In_{0.2}Ga_{0.8}As$,	undoped
Waveguide	0.3 μm,	GaAs,	undoped
p-type emitter	1.5 μm,	$Al_{0.3}Ga_{0.7}As$,	Be-doped $p = 3.5\times10^{17}$ cm^{-3}
Cap layer	0.25 μm,	GaAs,	Be-doped $p = 2\times10^{19}$ cm^{-3}

The design of the structure has been numerically simulated using commercial PICS 3D software [4] package from Crosslight Software Inc. The 20% indium content in the active layer and 60 Å thickness of the quantum well to obtain 980 nm RT emission have been found as appropriate. Both values have been confirmed by photoluminescence (PL) measurements taken on MBE as grown structures. Numerical calculations provided also the optimal length of the laser cavity and mesa width to be 700 and 200 μm, respectively. The laser mirrors remained uncoated and therefore their reflectivity was around 32% and assured approximately the same power emission from the front and rear sides of the laser.

The laser was mounted on a heat sink in *p*-type up configuration and placed on a stage with a thermoelectric cooler to stabilize its temperature during the experiment at 20°C with accuracy of 0.1°C. The spectra were taken for a laser driven by 1.5 A current pulses of 20 μs width. The schematic layout of the experimental set-up used for measurements of the time-resolved laser spectra map is shown in Fig. 1.

It was operated as follows. First, the monochromator (Carll Zeiss Jena SPM2) was set to an arbitrary chosen starting wavelength and a slit width was selected at 0.020 mm. Then, the light beam emitted by the laser was focused on the

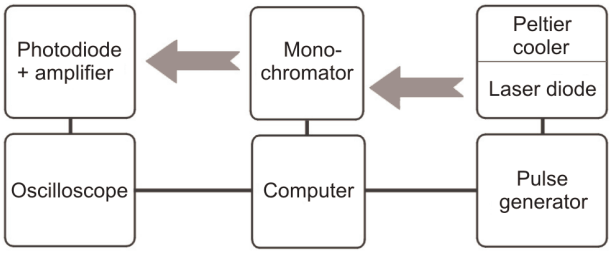

Fig. 1. Experimental set-up for measurements of the time-resolved laser spectra maps.

monochromator slit using two microscope objectives L_1 and L_2 (20× magnification, f = 1.4 mm, 0.4NA) mounted on the opto-mechanical system that allowed for a precise X, Y, Z movement. The optical output at the selected wavelength was measured by a typical Si photodiode. The electrical signal was subsequently amplified and afterwards was collected and visualized with an oscilloscope LeCroy 9361 300 MHz band. After that, the signal was stored in a computer. Next, the monochromator was set to the consecutive wavelength and the procedure was repeated until the full laser spectrum was registered. All stored data when plotted in 2D diagram form a complete time and spectrally resolved map.

3. Results and discussion

The main heat sources in a semiconductor laser are non-radiative recombination and Joule heating due to the electrical resistance of the semiconductor layers forming the laser. This heat is conducted away, mostly by the heat sink. Efficiency of this process depends on whether the laser was mounted *p*-up or *p*-down and the *p*-up configuration is evidently less effective. We applied it to have the heating of the laser active region more pronounced.

Any temperature increase of this region can be estimated by observing displacement of the center wavelength in the spectrum towards longer wavelength [5]. Both, the individual longitudinal modes and the spectrum envelope are shifting. To study these effects in the pulse operated lasers we applied the time-resolved laser spectra mapping technique described above and the results collected for 20 μs pulses are presented in Fig. 2. The colors of the races represent the level of the signal, respectively.

As can be seen from Fig. 2 the laser active region temperature was growing during the current pulse and the center wavelength of the spectrum was shifting correspondingly about 2 nm towards longer wavelengths. Assuming that for longitudinal modes [5] $\mathrm{d}\lambda/\mathrm{d}T$ = 0.26 nm/K, we calculate the investigated laser temperature increase to be of 9 K within 20 μs pulse.

It is important to note that temperature of the active region in the operating laser has not been achieving a stable level stabilization before the end of the pulse and therefore the output power dramatically decreased with duration time of the driving

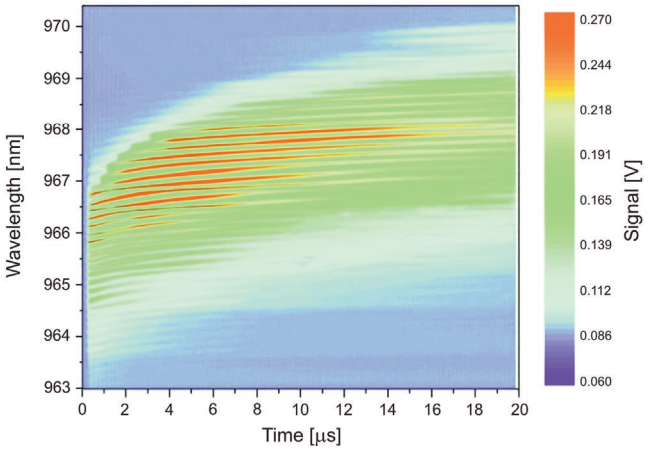

Fig. 2. High-resolution time-resolved laser spectra map collected within 20 μs pulse duration time. All spectra shifts towards longer wavelengths.

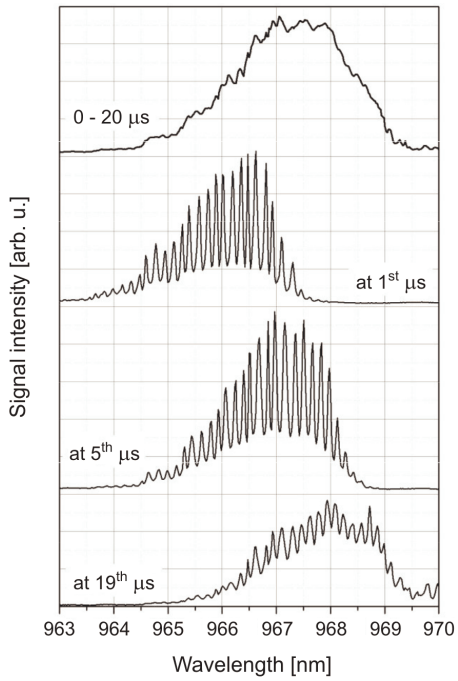

Fig. 3. Spectra extracted from the high-resolution time-resolved laser spectra map shown in Fig. 2. Particular curves correspond to different time points within duration time of the pulse. The first thickest curve represents cumulative spectrum collected by whole pulse time duration.

current pulse. A cross-section at the chosen time moment on this graph gives an extracted laser spectrum measured at this particular moment as shown in Fig. 3.

Figure 3 displays consecutive cumulated spectra, each representing particular time point within the pulse. The thick upper line is a sum of all measured curves. Because

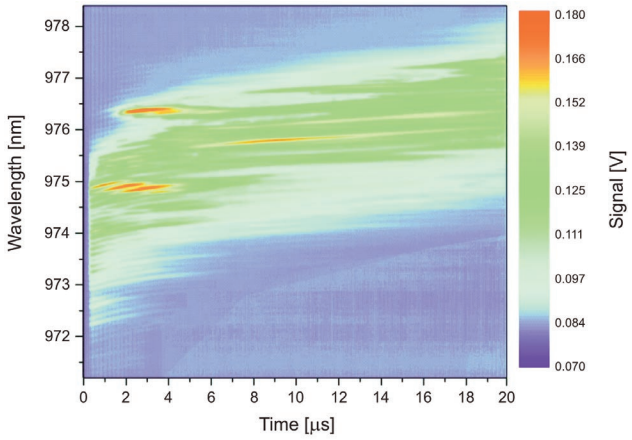

Fig. 4. Example of time-resolved laser spectra map collected within 20 μs pulse duration time. The laser was operated in an unstable fashion.

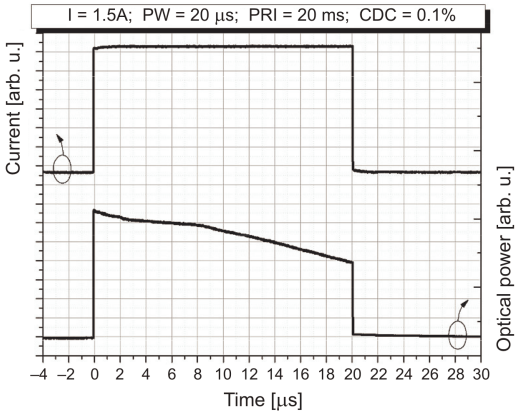

Fig. 5. Light output power (bottom) and current pulse (top) plotted *vs.* time.

of the random character of the spectra component the individual modes have been smeared in this curve. Temperature rise effects are however made clearly evident.

It should be mentioned that the graph shown in Fig. 2 has been obtained for a standard well operating laser. One should be aware that such graph might come out immensely distorted if the laser operates in an unstable fashion, mainly due to intensive filamentary action. An example of such graph is displayed in Fig. 4.

As has been mentioned, the light output measured within the pulse duration is dropping with the elapsing time. This effect is shown in Fig. 5 and it indicates that such diagram may be very helpful in assessment of the laser thermal, optical and electrical properties.

4. Summary

The temperature growth in the active region of the pulse-operated laser strongly affects performance of the device. The presented time-resolved laser spectra mapping technique has proved to be a useful tool in evaluation of the design and fabrication quality of the high power broad contacts lasers.

References

[1] LAFF R.A., COMERFORD L.D., CROW J.D., BRADY M.J., *Thermal performance and limitations of silicon-substrate packaged GaAs laser arrays*, Applied Optics **17**(5), 1978, pp. 778–84.

[2] DYMENT J.C., CHENG Y.C., SPRINGTHORPE A.J., *Temperature dependence of spontaneous peak wavelength in GaAs and $Ga_{1-x}Al_xAs$ electroluminescent layers*, Journal of Applied Physics **46**(4), 1975, pp. 1739–43.

[3] MANSANARES A.M., ROGER J.P., FOURNIER D., BOCCARA A.C., *Temperature field determination of InGaAsP/lnP lasers by photothermal microscopy: evidence for weak nonradiative processes at the facets*, Applied Physics Letters **64**(1), 1994, pp. 4–6.

[4] *PICS 3D Instruction Manual*, Crosslight Software Inc., CA 1998.

[5] MENZEL U., BARWOLFF A., ENDERS P., ACKERMANN D., PUCHERT R., VOSS M., *Modelling the temperature dependence of threshold current, external differential efficiency and lasing wavelength in QW laser diodes*, Semiconductor Science and Technology **10**(10), 1995, pp. 1382–92.

Received June 6, 2005
in revised form October 14, 2005